Technical University of Denmark

DTU

Lattice-matched Cu2ZnSnS4/CeO2 solar cell with open circuit voltage boost

Crovetto, Andrea; Yan, Chang; Iandolo, Beniamino; Zhou, Fangzhou; Stride, John; Schou, Jørgen; Hao, Xiaojing; Hansen, Ole

DTU Library
Technical Information Center of Denmark

Lattice-matched Cu2ZnSnS4/CeO2 solar cell with open circuit voltage boost

Andrea Crovetto, Chang Yan, Beniamino Iandolo, Fangzhou Zhou, John Stride, Jørgen Schou, Xiaojing Hao, and Ole Hansen

---

Articles you may be interested in

Band slope in CdS layer of ZnO:Ga/CdS/Cu2ZnSnS4 photovoltaic cells revealed by hard X-ray photoelectron spectroscopy
Appl. Phys. Lett. **109**, 203902 (2016); 10.1063/1.4967979

Band offset at the heterojunction interfaces of CdS/ZnSnP2, ZnS/ZnSnP2, and In2S3/ZnSnP2
J. Appl. Phys. **119**, 193107 (2016); 10.1063/1.4950882

In situ process monitoring during multistage coevaporation of Cu2ZnSnS4 thin films
J. Vac. Sci. Technol. A **33**, 021206 (2015); 10.1116/1.4906787

Towards a CdS/Cu2ZnSnS4 solar cell efficiency improvement: A theoretical approach
Appl. Phys. Lett. **105**, 233501 (2014); 10.1063/1.4903826

Effects of potassium doping on solution processed kesterite Cu2ZnSnS4 thin film solar cells
Appl. Phys. Lett. **105**, 223903 (2014); 10.1063/1.4903500

Lattice-matched Cu₂ZnSnS₄/CeO₂ solar cell with open circuit voltage boost

Andrea Crovetto,[1,2,a)] Chang Yan,[2] Beniamino Iandolo,[3] Fangzhou Zhou,[2] John Stride,[4] Jørgen Schou,[5] Xiaojing Hao,[2,b)] and Ole Hansen[1,6]

[1]DTU Nanotech, Technical University of Denmark, DK-2800 Kongens Lyngby, Denmark
[2]School of Photovoltaic and Renewable Energy Engineering, University of New South Wales, Sydney, NSW 2052, Australia
[3]DTU CEN, Center for Electron Nanoscopy, DK-2800 Kongens Lyngby, Denmark
[4]School of Chemistry, University of New South Wales, Sydney, NSW 2052, Australia
[5]DTU Fotonik, Technical University of Denmark, DK-4000 Roskilde, Denmark
[6]V-SUSTAIN, Villum Center for the Science of Sustainable Fuels and Chemicals, Technical University of Denmark, DK-2800 Kongens Lyngby, Denmark

We report a reproducible enhancement of the open circuit voltage in Cu₂ZnSnS₄ solar cells by introduction of a very thin CeO₂ interlayer between the Cu₂ZnSnS₄ absorber and the conventional CdS buffer. CeO₂, a non-toxic earth-abundant compound, has a nearly optimal band alignment with Cu₂ZnSnS₄ and the two materials are lattice-matched within 0.4%. This makes it possible to achieve an epitaxial interface when growing CeO₂ by chemical bath deposition at temperatures as low as 50 °C. The open circuit voltage improvement is then attributed to a decrease in the interface recombination rate through formation of a high-quality heterointerface. *Published by AIP Publishing.* [http://dx.doi.org/10.1063/1.4971779]

Cu₂ZnSn(S,Se)₄ compounds are among the materials that are currently considered as potentially suitable for terawatt-scale solar energy production. The pure-sulfide material Cu₂ZnSnS₄ (CZTS) is particularly interesting because it avoids the relatively scarce element Se, and it has a larger band gap (1.5 eV), which is appropriate both for a single-junction solar cell and for a top absorber in a tandem solar cell architecture.[1] Even though its highest reported power conversion efficiency so far (9.1%) was achieved with a CdS heterointerface partner, or buffer layer,[2] interface recombination is still the dominant voltage loss mechanism in the solar cell,[3] which suggests that CdS is not the ideal partner of CZTS. Despite promising results achieved with (Zn,Cd)S and (Zn,Sn)O buffer layers,[4,5] no alternative materials to date have outperformed the highest efficiency[2] or the highest open circuit voltage[6] achieved with a CdS heterojunction partner.

The open circuit voltage V_{oc} of a solar cell limited by interface recombination can be expressed as

$$V_{oc} = \frac{E_i}{q} - \frac{kT}{q} \ln\left(\frac{qS_p N_v}{J_{sc}}\right) \qquad (1)$$

for a p-type absorber with an inverted heterointerface, i.e., with holes as minority carriers at the interface.[7] E_i is the interface band gap, q is the elementary charge, k is the Boltzmann's constant, T is the temperature, N_v is the effective density of states in the valence band, J_{sc} is the short circuit current, and S_p is the interface recombination velocity of holes. By modeling interface recombination as Shockley-Read-Hall recombination through a single interface defect level, S_p can be expressed as

$$S_p = N_i \sigma_p v_{th}, \qquad (2)$$

where N_i is the area density of interface defects, σ_p is a cross section describing how efficiently the holes are captured by the defect, and v_{th} is the thermal velocity.[8]

Eqs. (1) and (2) show that decreasing the interface defect density N_i can be a way to improve the open circuit voltage in a solar cell limited by interface recombination. By analogy to high-efficiency solar cell technology based on III–V semiconductors,[9] this can be achieved by ensuring epitaxial growth of the buffer material on the absorber material. In the absence of epitaxial growth, a large density of atomic dislocations will exist at the interface, which leads to formation of allowed electronic states within the interface bandgap, thus increasing N_i and enhancing interfacial Shockley-Read-Hall recombination. Epitaxial growth is facilitated by a small lattice mismatch between the two heterojunction materials.[9] While CdS has a reasonably small lattice mismatch with the absorber materials Cu(In,Ga)Se₂ (∼1.5%) and Cu₂ZnSnSe₄ (∼2.4%), its mismatch with CZTS is much larger (∼7%). A high value of N_i can therefore be anticipated at the CZTS/CdS interface.

To address this problem, we carried out an initial investigation of the non-toxic, earth abundant material[10] CeO₂ as a heterojunction partner of CZTS. CeO₂ has a nearly perfect lattice match[11] with CZTS (lattice constant of CZTS: 5.43 Å; lattice constant of CeO₂: 5.41 Å; thus a lattice mismatch under 0.4%). This opens the possibility for a high-quality epitaxial interface, which may alleviate the interface recombination problem. CeO₂ also has a wide indirect bandgap[12,13] of 3.3 eV, which minimizes parasitic light absorption. We note that, based on Eq. (1), the lattice mismatch at the CeO₂/CdS interface is not expected to limit V_{oc}, since E_i is much larger at the CeO₂/CdS interface than at the CZTS/CeO₂ interface.

CZTS films were prepared by co-sputtering Cu/ZnS/SnS precursors on Mo-coated soda lime glass using a magnetron

a)Electronic mail: ancro@nanotech.dtu.dk
b)Electronic mail: xj.hao@unsw.edu.au

sputtering system (AJA International, Inc., model ATC-2200) as presented in detail before.[14] Two types of elemental compositions were targeted in different CZTS precursors within the same batch: the first (C1) with Cu/Sn = 1.9 and Zn/Sn = 1.25; the second (C2) with Cu/Sn = 1.8 and Zn/Sn = 1.25. C1 and C2 were chosen because the final solar cell efficiency is very sensitive to the sample stoichiometry, especially to the Cu/Sn ratio.[15] These precursors were then annealed using Rapid Thermal Processor (AS-One 100) in a S- and Sn-containing atmosphere at 560 °C. The S atmosphere compensates for S substoichiometry in the precursors and the addition of Sn stabilizes CZTS against decomposition reactions.[16] CeO_2 films were deposited on CZTS by chemical bath deposition (CBD) at 50 °C in a weakly acidic solution (pH:6) containing 10 mM $Ce(CH_3COO)_3$ and 5 mM $KClO_3$ in Milli-Q water under mild stirring. The expected chemical reactions resulting in thin film deposition are those presented in previous work.[17] CdS (60 nm) was deposited by CBD with a previously described process.[14] ZnO (60 nm) and indium tin oxide (ITO, 200 nm) layers were deposited by RF magnetron sputtering, followed by an Al contact grid. No anti-reflection coating was applied. The total area of the final cells (0.23 cm^2) was defined by mechanical scribing. Three different solar cell architectures were fabricated in this work as shown in Fig. 1. In the first architecture (A1), CdS is completely replaced by a stand-alone 30 nm CeO_2 buffer layer deposited with a 100 min process. In the second architecture (A2), a thin CeO_2 layer of estimated thickness between 1 and 5 nm is inserted between CZTS and the standard CdS buffer layer using a 10–20 min deposition process. The reference architecture (Fig. 1) is a conventional CZTS solar cell structure without CeO_2. Only very weak n-type conductivity[18] has been reported for CeO_2 and, in fact, the resistivity of the films synthesized in this work was too high to be measured with conventional four-point probe apparatus. Therefore, the CeO_2 layer in the solar cell can be regarded as completely depleted. In the case of architecture A2, the CeO_2 layer is so thin that it is not expected to modify significantly the original electric field profile of the reference architecture.

Scanning electron microscope images were taken with a FEI-Nova NanoSEM 450 instrument at 2 kV beam voltage. High-resolution bright-field transmission electron microscope images (HRTEM) were taken with a FEI-Titan 80–300 TEM, at 300 kV beam voltage. X-ray photoelectron spectroscopy (XPS) was performed with a Thermo Scientific

K-Alpha instrument with a monochromatized Al K_α X-ray source. The binding energy scale was calibrated using the adventitious C 1s peak at 284.8 eV. An electron flood source was employed to limit the charging effects in CeO_2.[19] CeO_2 was found by others to be reduced to Ce_2O_3 both under prolonged X-ray exposure[20] and under ion beam sputtering.[19] Indeed, by inspection of the Ce 3d spectrum and of the valence band edge, reduction effects were evident in our films even at the lowest ion beam energy (200 eV) available in the XPS setup. Therefore, no sputter cleaning was performed on our samples. XPS data analysis was performed with the Avantage 5.948 software (Thermo Scientific). Current-voltage (JV) characteristics on finished devices were measured under AM 1.5G illumination with a solar simulator from PV Measurement and a Keithley 2400 source meter calibrated with a standard Si reference.

Before discussing the solar cell results, we want to answer some basic questions about the quality of deposited CeO_2 films. The first question is adhesion. By depositing CeO_2 on glass/Mo substrates, it was found that the films deposited from a solution with a $KClO_3$ concentration of 10 mM or above were easily peeled off by scotch tape. However, already at a $KClO_3$ concentration of 5 mM, the films were strongly adherent with no peel-off by repeated scotch tape application. A $KClO_3$ concentration of 5 mM was therefore chosen for the deposition process. The maximum CeO_2 thickness on CZTS that could be achieved in a single chemical bath deposition run was about 30 nm with a 100 min process (Fig. S1(a), supplementary material).

The second question is whether the deposited film indeed consists of the desired CeO_2 material. The fast Fourier transform (FFT) of cross-sectional TEM images of the deposited film yields a pattern that is compatible with CeO_2 and not with the main competing phase Ce_2O_3 (Fig. 2(c)). However, the TEM analysis involves very small regions (few nm). Raman spectroscopy was then performed over a much larger analysis area (about 2 μm diameter). Only one additional Raman peak at 461 cm^{-1} was revealed on CZTS/CeO_2 bilayers compared to a bare CZTS spectrum (Fig. S2, supplementary material). The peak corresponds to the first-order-allowed Raman mode of CeO_2, with a small red shift due to size effects.[21] Finally, XPS characterization was performed over an even larger analysis area (about 400 μm diameter). All the XPS peaks corresponding to Ce 3d core levels were fitted and attributed to either CeO_2 or Ce_2O_3 according to reference spectra[22] (Fig. S3, supplementary material). The fraction of CeO_2 present in the deposited film is estimated as 70.4% with this method. Hence, some Ce_2O_3 inclusion should be expected. Since Ce_2O_3 is not lattice-matched to CZTS, and it has a band gap[13] almost 1 eV lower than that of CeO_2, we assume that Ce_2O_3 inclusions promote interface recombination and reduce the open circuit voltage enhancement that could be achieved with a pure CeO_2 layer.

The third question is whether the deposited film provides a complete coverage of the underlying CZTS layer. SEM images of a 30 nm-thick CeO_2 film (Fig. 3) show some non-uniform coverage in correspondence of CZTS grain boundaries and some smaller isolated dips in the CeO_2 film profile, which may be interpreted as pinholes. The area
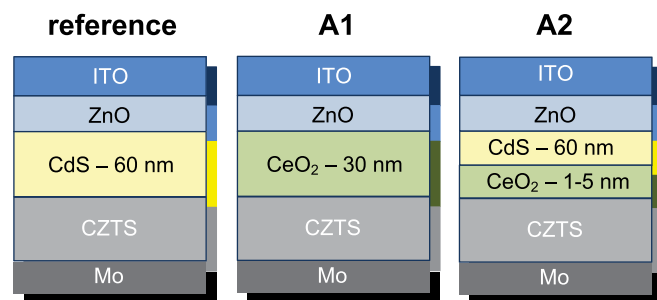

FIG. 1. Schematic drawing of the A1 architecture with a 30 nm stand-alone CeO_2 buffer layer and the A2 architecture with a 1–5 nm CeO_2 interlayer between CZTS and CdS. The reference architecture is a standard CZTS solar cell structure.
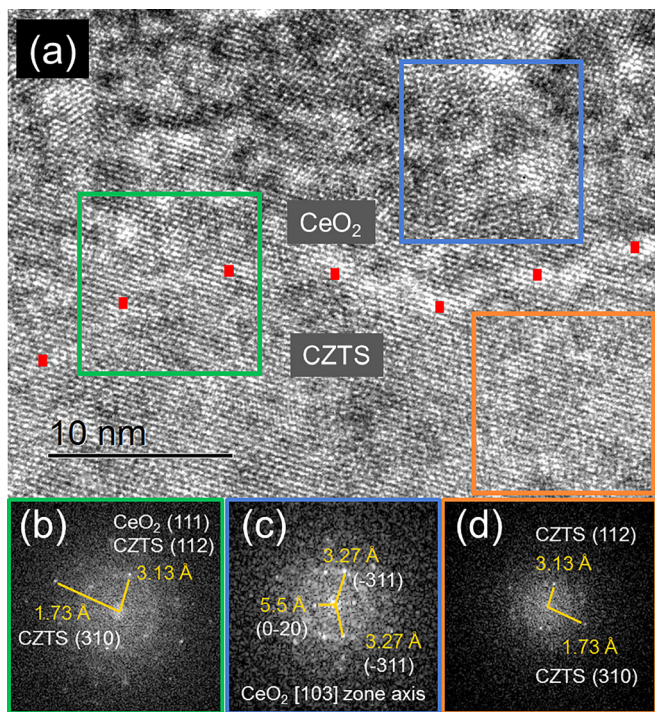
FIG. 2. (a) Cross-sectional HRTEM image across the interface between CeO_2 (top) and CZTS (bottom). (b) FFT of a selected region across the interface. A reflection at 3.13 Å is visible, corresponding to the distance between (111) planes of CeO_2 and between the (112) planes of CZTS. (c) FFT of a selected region within CeO_2. The diffractogram can be indexed as a CeO_2 crystal along with [103] as the zone axis. (d) FFT of a selected region within CZTS. Reflections corresponding to the (112) and (310) planes are visible.

fraction of CZTS that is covered by CeO_2 can be estimated by comparing the peak intensity of Ce, Cu, Zn, and Sn core levels by XPS, as explained in the supplementary material. The covered area is then estimated as 62%, 94%, and 95% for the films deposited for 20, 60, and 90 min, with estimated thicknesses of 1–5, 15, and 25 nm, respectively. Thus, it seems as if the very thin films (20 min deposition time) employed in architecture A2 may have rather poor coverage. However, in that case the CeO_2 thickness is comparable to the XPS probing depth (about 2 nm). Therefore, part of the CZTS signal is likely to originate from CZTS buried under CeO_2 so that the covered fraction is in reality higher. The consequence of incomplete coverage is simply the coexistence of CZTS/CeO_2 and CZTS/CdS heterojunctions in parallel to the solar cells.

The fourth question is whether CeO_2 forms an epitaxial interface with CZTS, as may be expected by their excellent
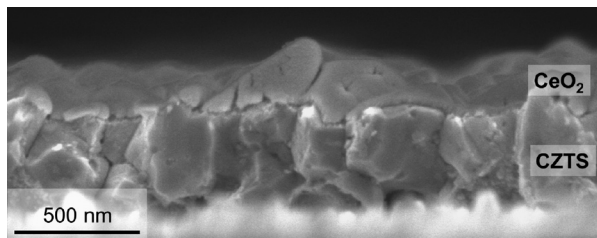

FIG. 3. The cross sectional SEM image of a CeO_2 film grown on CZTS used for architecture A1. The film is about 30 nm thick, which is the maximum thickness that could be achieved with a single CBD process in this work. Some scattered pinholes and inhomogeneous coverage of the grain boundaries are seen.

lattice match. The HRTEM image in Fig. 2(a) shows that the atomic arrangement on the CZTS side continues on the CeO_2 side for a few nm, thus demonstrating that an epitaxial interface *can* be achieved despite the low deposition temperature. Analysis of the FFT pattern across the interface (Fig. 2(b)) reveals that epitaxy occurs along the CZTS(112)-CeO_2(111) direction, similar to what was recently observed on a CZTS/CdS interface.[23] A few nm away from the interface, CeO_2 is nanocrystalline with an average grain size less than 5 nm, as inferred from TEM images (Fig. 2(a)) and by quantitative analysis of Raman peak broadening (Fig. S2, supplementary material). We emphasize, however, that epitaxial growth was *not* observed at most interface locations imaged by TEM in this work, as shown for example, in Fig. S1(b), supplementary material.

The fifth and final question is the band alignment of CeO_2 with CZTS. It is well known that a moderate spike-like conduction band offset (CBO) at the heterointerface, in the 0–0.4 eV range, is optimal as it reduces interface recombination without blocking photocurrent transport.[24] The valence band offset (VBO) was estimated by XPS as shown in Fig. 4. The experimental (bulk) band gaps of the two materials were then added to the VBO to finally obtain a CBO of -0.12 ± 0.20 eV. For the CeO_2 indirect gap, we used a value of 3.3 ± 0.1 eV measured by the internal photoemission yield.[12] The extracted CBO is only slightly below the optimal range, and it is actually more favorable than the previously measured CZTS/CdS band offset.[25] Considering the many possible sources of error in the measurement, including the use of as-deposited surfaces for analysis, this is considered as a promising result. We also note that the CeO_2 Fermi level lies about 2.7 eV above the valence band, which indicates that CeO_2 is n-type in the analysis region, similar to previous reports.[22,26]
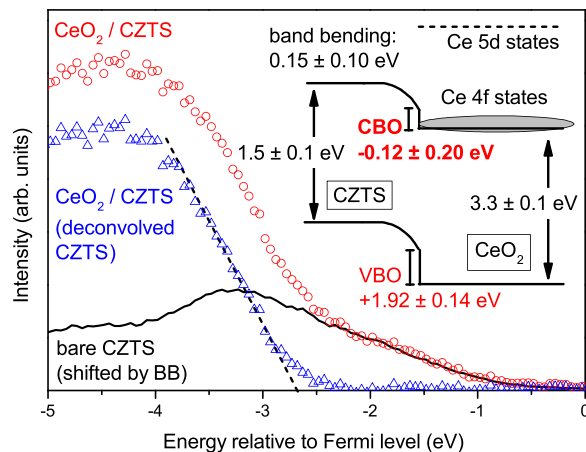

FIG. 4. CZTS/CeO_2 band alignment extracted by XPS. The valence band maximum (VBM) of CZTS with respect to the Fermi level is -0.60 ± 0.10 eV in a bare CZTS sample and -0.75 ± 0.10 eV in a CZTS sample coated with a thin CeO_2 layer (20 min deposition time, red circles). From this, band bending (BB) in CZTS is estimated as 0.15 ± 0.10 eV. This is also confirmed from the average shift in the Cu 2p, Zn 2p, and Sn 3d core levels between the bare CZTS sample and the CeO_2/CZTS sample. Shifting the XPS spectrum of the bare CZTS sample by the BB (black line) allows deconvolution of the CeO_2 valence band signal (blue triangles), located -2.67 ± 0.10 eV below the Fermi level. The shifted spectrum of bare CZTS (black line) fits well with the CeO_2/CZTS spectrum until the onset of the CeO_2 valence band, as expected.
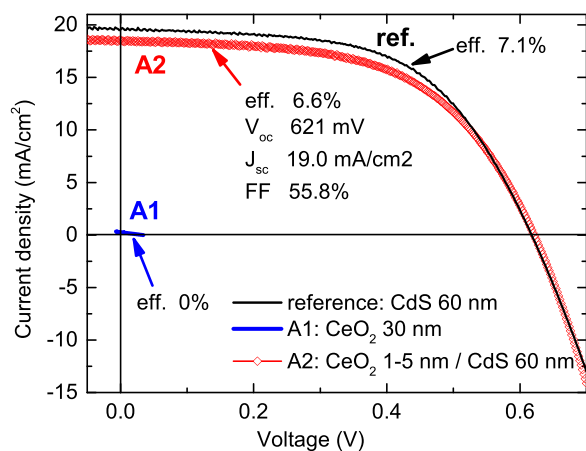
FIG. 5. Illuminated current-voltage characteristics of the best solar cells with the A1 and A2 architectures, together with the best solar cell with the reference architecture.

The current-voltage characteristics of the three best solar cells fabricated with the three different architectures are shown in Fig. 5. A small improvement in open circuit voltage is achieved by architecture A2 with respect to the reference architecture. The accompanying degradation in short circuit current will be discussed in the following. Interestingly, the statistics shown in Fig. 6 indicate that the V_{oc} boost is reproducible over two separate batches (i) and (ii) regardless of precursor composition (C1 or C2). In all those cases, the open circuit voltage of the solar cells with A2 architecture is always between 20 mV and 100 mV higher than in the corresponding solar cells with the standard CdS architecture. Additional statistics in Fig. S6 (supplementary material) confirm this trend. The highest open circuit voltage achieved in this study with the A2 architecture was 641 mV, and the highest efficiency was 6.6% (Fig. 5). Conversely, complete current blocking and no photovoltaic effect was observed in the solar cells with a stand-alone CeO_2 buffer layer (architecture A1 in Fig. 5).

To interpret these results, we refer to the band structure of CeO_2.[13] What has been referred to as the "conduction band" in this work is a band consisting of highly localized Ce 4f states, 3.3 eV above the valence band as mentioned before.[12] However, localization of states in this band implies

that the electron effective mass is very high, and hence the electron mobility is very low. This can be inferred by a nearly complete lack of dispersion of those states in reciprocal space.[13] For this reason, a band consisting mostly of Ce 5d states, which lies about 6 eV above the valence band has lighter effective masses, is often quoted as the conduction band of CeO_2. From our band alignment study (Fig. 4), we found that the 4f band has a nearly optimal CBO with the CZTS conduction band, while the 5d band lies at a much higher energy. Then, we can attribute the complete lack of photocurrent in architecture A1 to the very poor transport properties of the 4f band. A 30 nm CeO_2 layer is therefore thick enough to completely impede electron transport. Instead, when CeO_2 is very thin as in architecture A2 (1–5 nm), short circuit current and fill factor losses are greatly diminished and in some cases eliminated (Fig. 5 and S5, supplementary material). This is possibly due to tunneling-based transport between the CZTS and CdS conduction bands through the thin interlayer. Residual current losses, as in Fig. 5, are probably due to thickness inhomogeneity of CeO_2, or to the fact that an even thinner layer is necessary. Growth of CeO_2 by atomic layer deposition may be beneficial in this respect.

We conclude that inserting a thin lattice-matched CeO_2 layer between CZTS and CdS alleviates interface recombination and results in a reproducible open circuit voltage boost in the solar cell. This is attributed to the formation of a high-quality $CZTS/CeO_2$ heterointerface, with instances of epitaxial growth observed in some regions. We suggest that the open circuit voltage could be further improved if epitaxy could be obtained on a larger scale, if Ce_2O_3 inclusions could be decreased, and if the surface coverage could be improved. Etching the CZTS surface immediately prior to CeO_2 deposition may facilitate the formation of an epitaxial interface. It should be kept in mind that the very large electron effective mass in the CeO_2 conduction band puts a severe constraint on the maximum thickness of the CeO_2 film, which should only be a couple of nm thick in order to avoid the dramatic current losses.

See supplementary material for additional TEM images, phase analysis of the CeO_2 layer, compositional analysis across the interface, estimation of CeO_2 coverage, and more detailed statistics on the solar cell parameters for the reference architecture and architecture A2.
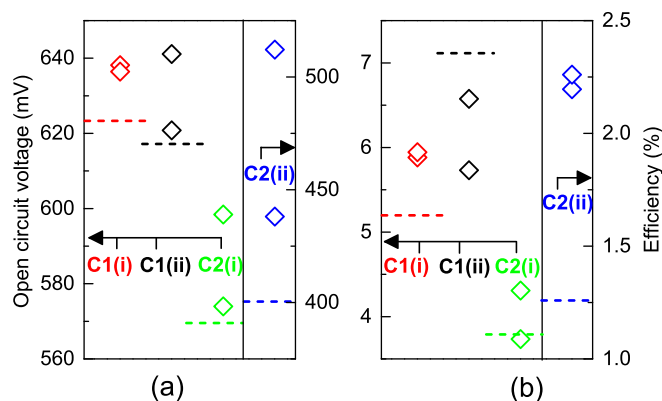
FIG. 6. Comparison of open circuit voltage (a) and conversion efficiency (b) between solar cells with the A2 architecture (diamond data points) and a reference solar cell with a pure CdS buffer layer (dashed line) within the same batch. C1 and C2 are two different CZTS compositions; (i) and (ii) are two different batches. Each data point represents the highest-efficiency solar cell within a chip containing 12 devices.

[1]M. A. Green, Nat. Energy **1**, 1 (2016).
[2]S. Tajima, T. Itoh, H. Hazama, K. Ohishi, and R. Asahi, Appl. Phys. Express **8**, 082302 (2015).

[3]M. Courel, J. A. Andrade-Arvizu, and O. Vigil-Galán, Appl. Phys. Lett. **105**, 233501 (2014).

[4]K. Sun, C. Yan, F. Liu, J. Huang, F. Zhou, J. A. Stride, M. Green, and X. Hao, Adv. Energy Mater. **6**, 1600046 (2016).

[5]C. Platzer-Björkman, C. Frisk, J. K. Larsen, T. Ericson, S.-Y. Li, J. J. S. Scragg, J. Keller, F. Larsson, and T. Törndahl, Appl. Phys. Lett. **107**, 243904 (2015).

[6]H. Hiroi, N. Sakai, T. Kato, and H. Sugimoto, in *2013 IEEE 39th Photovoltaic Specialists Conference (PVSC)* (IEEE, 2013), pp. 0863–0866.

[7]U. Rau and H. Schock, Appl. Phys. A **69**, 131 (1999).

[8]S. Sze and K. K. Ng, *Physics of Semiconductor Devices* (Wiley, 2004), p. 68.

[9]D. J. Friedman, J. M. Olson, and S. Kurtz, in *Handbook of Photovoltaic Science and Engineering*, 2nd ed., edited by A. Luque and S. Hegedus (John Wiley & Sons, Ltd., Chichester, UK, 2011), Chap. 8, p. 338.

[10]U.S. Geological Survey, Fact Sheet 087-02, 2005.

[11]M. Yashima, S. Kobayashi, and T. Yasui, Solid State Ionics **177**, 211 (2006).

[12]V. V. Afanas'ev, S. Shamuilia, A. Stesmans, A. Dimoulas, Y. Panayiotatos, A. Sotiropoulos, M. Houssa, and D. P. Brunco, Appl. Phys. Lett. **88**, 132111 (2006).

[13]R. Gillen, S. J. Clark, and J. Robertson, Phys. Rev. B **87**, 125116 (2013).

[14]C. Yan, F. Liu, K. Sun, N. Song, J. A. Stride, F. Zhou, X. Hao, and M. Green, Sol. Energy Mater. Sol. Cells **144**, 700 (2016).

[15]C. Yan, K. Sun, F. Liu, J. Huang, F. Zhou, and X. Hao, Sol. Energy Mater. Sol. Cells **160**, 7 (2017).

[16]A. Redinger, D. M. Berg, P. J. Dale, and S. Siebentritt, J. Am. Chem. Soc. **133**, 3320 (2011).

[17]H. Unuma, T. Kanehama, K. Yamamoto, K. Watanabe, T. Ogata, and M. Sugawara, J. Mater. Sci. **38**, 255 (2003).

[18]R. N. Blumenthal and R. L. Hofmaier, J. Electrochem. Soc. **121**, 126 (1974).

[19]D. Mullins, S. Overbury, and D. Huntley, Surf. Sci. **409**, 307 (1998).

[20]E. Paparazzo, G. M. Ingo, and N. Zacchetti, J. Vac. Sci. Technol. A **9**, 1416 (1991).

[21]G. Graham, W. Weber, C. Peters, and R. Usmen, J. Catal. **130**, 310 (1991).

[22]Y. Zhu, N. Jain, M. K. Hudait, D. Maurya, R. Varghese, and S. Priya, J. Vac. Sci. Technol. B **32**, 011217 (2014).

[23]F. Liu, C. Yan, J. Huang, K. Sun, F. Zhou, J. A. Stride, M. A. Green, and X. Hao, Adv. Energy Mater. **6**, 1600706 (2016).

[24]M. Gloeckler and J. Sites, Thin Solid Films **480–481**, 241 (2005).

[25]C. Yan, F. Liu, N. Song, B. K. Ng, J. A. Stride, A. Tadich, and X. Hao, Appl. Phys. Lett. **104**, 173901 (2014).

[26]H. F. Wardenga and A. Klein, Appl. Surf. Sci. **377**, 1 (2016).